Fullerene-C_{60} and PCBM as interlayers in regular and inverted lead-free PSCs using $CH_3NH_3SnI_3$: An analysis of device performance and defect density dependence by SCAPS-1D

Vívian Helene Diniz Araújo, Ana Flávia Nogueira
Juliana Cristina Tristão and Leandro José dos Santos

1 Electronic Supplementary Information (ESI)

Table S1: Input parameters of PEDOT:PSS, Spiro-MeOTAD and TiO_2 for the subsection 3.1 simulations.

Parameters/Materials	**PEDOT:PSS [2]**	**Spiro-MeOTAD [1]**	**TiO_2 [1]**
Thickness (nm)	200	200	30
E_g (eV)	2.20	3.17	3.20
χ(eV)	2.90	2.05	4.26
εr	3.00	3.00	9.00
N_c (cm^{-3})	$2.2x10^{15}$	2.50×10^{18}	2.00×10^{18}
N_v (cm^{-3})	$1.8x10^{18}$	1.80×10^{19}	1.80×10^{19}
μ_e ($cm^2V^{-1}s^{-1}$)	1.00×10^{-2}	2.00×10^{-4}	20
μ_h ($cm^2V^{-1}s^{-1}$)	2.00×10^{-4}	2.00×10^{-4}	10
N_A (cm^{-3})	$1.0x10^{15}$	1.00×10^{17}	-
N_D (cm^{-3})	-	–	1.00×10^{16}
N_t (cm^{-3})	$1.0x10^{14}$	1.00×10^{13}	1.00×10^{15}

Table S2: PCE of simulated PSCs using different HTLs and ETLs for n-i-p and p-i-n PSCs with N_t=4.5x10^{17} cm^{-3}. The perovskite thickness was 350 nm and the ETL/HTL thickness was 30 nm and 200 nm, respectively.

HTL/ETL Regular PSC	**TiO_2**	**ZnO**	**HTL/ETL Inverted PSC**	**TiO_2**	**ZnO**
Spiro-MeOTAD	6.12%	6.40%	PEDOT:PSS	1.17%	1.10%
CuI	6.54%	6.89%	CuI	1.06%	1.35%

Table S3: Influence of MASI thickness in simulated PSCs with CuI and ZnO as HTL/ETL (30 nm) in regular and inverted configurations, using N_t=4.5x10^{17} cm^{-3}.

PSC n-i-p	**V_{oc} (V)**	**J_{sc} (mA/ cm^2)**	**FF (%)**	**PCE (%)**	**PSC p-i-n**	**V_{oc} (V)**	**J_{sc} (mA/cm^2)**	**FF (%)**	**PCE (%)**
CuI/MASI(150nm)/ZnO	0.66	17.20	49.97	5.70	CuI/MASI(150nm)/ZnO	0.65	15.35	37.25	3.72
CuI/MASI(200nm)/ZnO	0.68	17.53	54.60	6.53	CuI/MASI(200nm)/ZnO	0.65	10.87	43.00	3.05
CuI/MASI(250nm)/ZnO	0.68	18.28	54.40	6.81	CuI/MASI(250nm)/ZnO	0.64	8.42	45.24	2.45
CuI/MASI(300nm)/ZnO	0.68	18.61	53.96	6.88	CuI/MASI(300nm)/ZnO	0.63	6.57	44.83	1.86
CuI/MASI(350nm)/ZnO	0.68	18.69	53.82	6.89	CuI/MASI(350nm)/ZnO	0.62	4.96	45.12	1.38
CuI/MASI(400nm)/ZnO	0.68	18.71	53.79	6.90	CuI/MASI(400nm)/ZnO	0.61	3.73	45.79	1.03
CuI/MASI(450nm)/ZnO	0.68	18.71	53.79	6.90	CuI/MASI(450nm)/ZnO	0.59	2.83	46.57	0.78
CuI/MASI(500nm)/ZnO	0.68	18.71	53.79	6.90	CuI/MASI(500nm)/ZnO	0.58	2.17	47.34	0.60
CuI/MASI(550nm)/ZnO	0.68	18.72	53.78	6.90	CuI/MASI(550nm)/ZnO	0.57	1.68	48.03	0.46
CuI/MASI(600nm)/ZnO	0.68	18.72	53.78	6.90	CuI/MASI(600nm)/ZnO	0.56	1.33	48.66	0.36
CuI/MASI(650nm)/ZnO	0.68	18.72	53.78	6.90	CuI/MASI(650nm)/ZnO	0.55	1.06	49.23	0.28
CuI/MASI(700nm)/ZnO	0.68	18.72	53.77	6.90	CuI/MASI(700nm)/ZnO	0.54	0.85	49.72	0.23
CuI/MASI(750nm)/ZnO	0.68	18.72	53.77	6.90	CuI/MASI(750nm)/ZnO	0.53	0.69	50.19	0.18
CuI/MASI(800nm)/ZnO	0.68	18.72	53.77	6.90	CuI/MASI(800nm)/ZnO	0.52	0.57	50.58	0.15

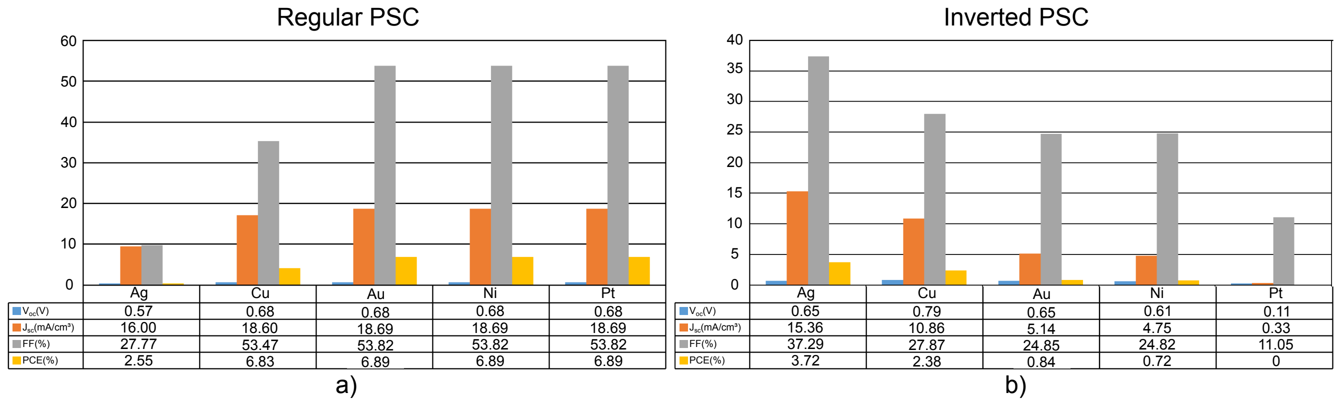

Figure S1: Output parameters varying back metal contacts in a) regular and b) inverted PSCs

Table S4: PCE in regular and inverted configurations using N_t=4.5x10^{13} cm^{-3}, with and without interlayers.

PSC	**Conf.**	**V_{oc} (V)**	**J_{sc} (mA/cm2)**	**FF (%)**	**PCE (%)**
CuI/MASI/ZnO	n-i-p	1.02	33.81	83.13	28.64
CuI/MASI/PCBM/ZnO	n-i-p	1.02	33.84	83.10	28.65
CuI/MASI/C_{60}/ZnO	n-i-p	1.02	33.92	77.78	26.92
CuI/MASI/ZnO	p-i-n	1.02	32.26	84.33	27.71
CuI/MASI/PCBM/ZnO	p-i-n	1.02	32.38	84.17	27.80
CuI/MASI/C_{60}/ZnO	p-i-n	1.02	32.26	79.01	25.99

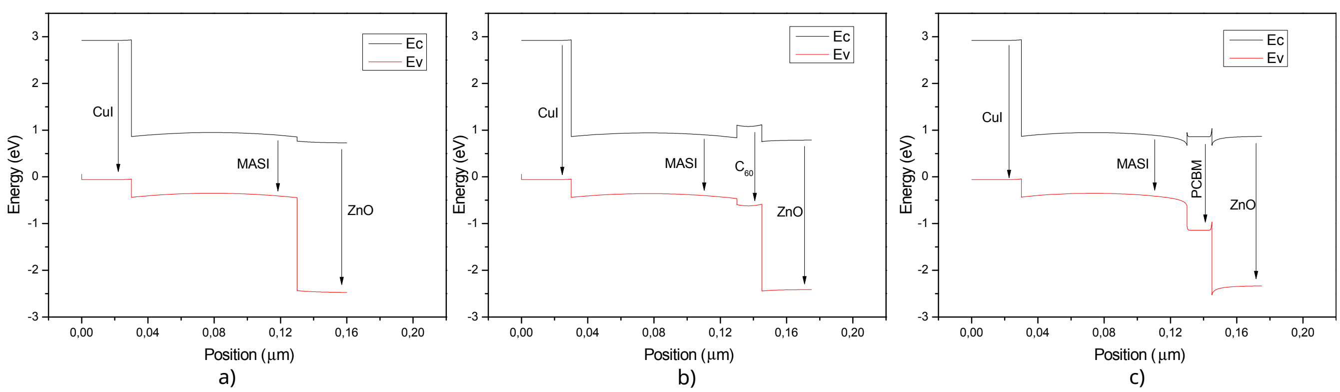

Figure S2: Energy diagram of simulated inverted PSCs. a) CuI/MASI/ZnO, b) CuI/MASI/C_{60}/ZnO, c) CuI/MASI/PCBM/ZnO, using N_t=4.5x10^{17} cm^{-3} and MASI thickness at 150 nm.

References

[1] H.-J. Du, W.-C. Wang, and J.-Z. Zhu. Device simulation of lead-free ch3nh3sni3 perovskite solar cells with high efficiency. *Chinese Physics B*, 25(10):108802, 2016.

[2] H. Sharma, V. K. Verma, R. C. Singh, P. K. Singh, and A. Basak. Numerical analysis of high-efficiency ch3nh3pbi3 perovskite solar cell with pedot: Pss hole transport material using scaps 1d simulator. *Journal of Electronic Materials*, pages 1–13, 2023.